Materials Today Communications 54 (2026) 115519

Contents lists available at ScienceDirect

Materials Today Communications

journal homepage: www.elsevier.com/locate/mtcomm

Formulation and characterization of sustainable materials for food packaging: PLA-PHB blends modified with different types of corn oil

Federico Barrino [a,*], Jaume Sempere-Torregrosa [b], Harrison de la Rosa-Ramírez [b], Federica Giuliano [a], María Dolores Samper [b]

[a] Department of Engineering, University of Palermo, Viale delle Scienze 6, Palermo 90128, Italy
[b] Institute of Materials Technology (IUTM), Universitat Politècnica de València (UPV), Alicante 46022, Spain

ARTICLE INFO

Keywords:
Food packaging
PLA-PHB
Film materials
Corn oil

ABSTRACT

Innovation in sustainable food packaging involves designing advanced bio-based materials that combine performance, biodegradability, and safety of use. In this study, a novel polymer blend based on PLA and PHB was developed, modified with 10 wt% epoxidized corn oil (Eo) and 2,5 wt% maleinized corn oil (Mo), two biofunctionalized additives obtained from renewable resources. This innovative combination was designed to enhance compatibility between polymeric phases, overcoming traditional limitations in fragility, poor processability, and barrier properties. The materials were characterized through FTIR-Fourier Transform Infrared Spectroscopy, contact angle measurements, mechanical tests, optical analyses, water vapor permeability, and suitability tests for food contact with fresh persimmon fruits. The results demonstrate a significant modification of surface chemistry, with an increase in hydrophobicity and improved phase dispersion. The mechanical properties exhibit an optimized balance between stiffness and deformability, which is essential for packaging applications. Furthermore, the transparency and optical properties were found to be stable, making it visually suitable for food packaging. Particularly innovative is the direct application test on persimmons, which highlighted the absence of visible migration or organoleptic alterations, suggesting excellent suitability for direct contact with fresh foods. This research therefore proposes a bioinspired and circular approach, valorizing agricultural by products to formulate functional, biodegradable, and safe materials, in line with European directives for increasingly sustainable packaging.

1. Introduction

1.1. Environmental challenges and the need for sustainable packaging

Food packaging today lies at the intersection of an environmental, technological, and socio-economic paradox. Conceived to ensure food protection, extend shelf life, and enable efficient distribution, packaging has evolved into a cornerstone of modern food systems. Yet, through the years, its very success has contributed significantly to a global pollution crisis.

Conventional petroleum derived plastics, while valued for their mechanical strength, optical clarity, and low cost, have become emblematic of convenience driven consumption. Their massive production and extremely short service life, often limited to a single use of only a few hours, stand in stark contrast with their long term environmental persistence, which can exceed four centuries. As microplastic contamination is now detected in oceans, soils, atmospheric dust, and even human biological tissues, the limitations of the fossil based packaging paradigm have become unequivocally evident [1,2]. At the same time, food systems face the parallel crisis of food waste. Every year, millions of tons of edible goods are discarded due to premature spoilage, inadequate packaging, temperature fluctuations during distribution, or inefficiencies throughout the supply chain. This loss entails not only an ethical dilemma in a world still facing hunger and malnutrition but also significant economic and environmental burdens, given that wasted food embodies squandered water, energy, and land resources [3,4].

The convergence of these issues underscores that packaging can no longer be understood as a passive containment system. Instead, it must become a multifunctional and adaptive technology capable of enhancing food preservation, mitigating waste, and reducing environmental footprint. Within this context, scientific and industrial interest in bio-based and biodegradable materials has intensified [5,6]. These materials

* Corresponding author.
E-mail address: federico.barrino@unipa.it (F. Barrino).

https://doi.org/10.1016/j.mtcomm.2026.115519
Received 9 April 2026; Received in revised form 31 May 2026; Accepted 8 June 2026
Available online 9 June 2026

promise to decouple packaging functionality from fossil resource dependence while enabling end of life scenarios that are more compatible with the principles of a circular economy [7].

1.2. PLA/PHB blends and compatibilization strategies

However, the transition from conventional plastics to sustainable alternatives is far from trivial. Bio-based materials must meet performance standards comparable to those of their petrochemical counterparts while offering advantages in compostability, safety, and renewability. Among the studied materials, biopolymers such as polylactic acid (PLA) and poly(3-hydroxybutyrate) (PHB) have emerged as leading candidates owing to their biological origin and inherent biodegradability under controlled conditions [8,9].

Despite their promise, neither PLA nor PHB alone meets all the functional requirements for food packaging applications. PLA, though widely available and industrially scalable, is intrinsically brittle and exhibits poor barrier properties against moisture. PHB, conversely, provides excellent barrier performance but suffers from thermal instability and a narrow processing window, which limit its commercial applicability. To address these shortcomings, blending PLA and PHB has been proposed as a strategy to synergistically enhance the performance of both biopolymers.

However, the immiscibility of the two polymers and their limited interfacial interactions pose challenges in achieving homogeneous and mechanically robust blends [10]. Advances in this field, therefore, require not merely physical mixing but profound engineering of the polymer network. Compatibilization strategies, particularly those relying on reactive, bio-based compounds have emerged as a promising route to stabilize the blend morphology and introduce tailored functionalities.

Table 1 summarizes representative PLA/PHB blend systems previously reported in the literature, highlighting the influence of different plasticizers and compatibilizers on the mechanical, thermal, and functional properties of the developed materials.

As observed, most previous studies mainly focused on improving the ductility and processability of PLA/PHB blends through conventional plasticization approaches. In contrast, the present work introduces chemically functionalized vegetable oils capable of simultaneously enhancing compatibility, moisture barrier properties, and functional performance, while maintaining the bio-based character of the system.

The present research embraces this approach by incorporating chemically modified vegetable oils into PLA/PHB blends with the objective of constructing a material blends that is simultaneously biodegradable, structurally performant, and functionally “smart.” Two natural origin additives, 10 wt% epoxidized corn oil (Eo) and 2,5 wt% maleinized corn oil (Mo), were selected due to their capacity to introduce reactive groups capable of interacting with PLA and PHB chains during processing [15]. These additives originate from an abundant and underutilized agricultural by-product, corn oil, which is upgraded through green functionalization pathways. Epoxidation and maleinization impart the oils with dual roles: as natural compatibilizers, they enhance interfacial adhesion and reduce phase separation between PLA and PHB; and as bio-based plasticizers, they enhance ductility, reduce brittleness, and improve overall processability. Through this strategy, the study aims not only to advance material performance but also to value agricultural side streams within a circular bioeconomy.

1.3. Experimental approach and objectives of the study

The experimental framework extends beyond classical material characterization to incorporate application-oriented testing that simulates realistic packaging conditions. Conventional analyses, including FTIR-Fourier Transform Infrared Spectroscopy to probe molecular interactions, contact angle measurements to assess surface wettability, mechanical testing to evaluate strength and deformability, optical characterization, and water vapor permeability assessments, offer fundamental insights into the structure property relationships of the developed bioplastics.

However, the inclusion of a direct food contact trial using fresh persimmon adds a crucial translational dimension. Persimmons represent a particularly challenging food matrix due to their high moisture content, sensitivity to external humidity, and susceptibility to rapid softening when stored under suboptimal conditions. Consequently, they serve as an effective model for evaluating packaging performance in real world scenarios. Monitoring visual, textural, and organoleptic changes in the fruit allows for an integrative assessment of the material’s breathability, moisture regulation capacity, and non-migratory behavior. Ultimately, this work aims to contribute to a paradigm shift in sustainable packaging research by demonstrating how agricultural byproducts, green chemistry techniques, and polymer blend engineering can be combined to design next generation materials.

Beyond simply replacing conventional plastics, the developed PLA/PHB oil bioplastics aspire to embody a new philosophy of packaging: one that protects the food it contains, aligns with the principles of a circular economy, minimizes ecological burden, and provides functional advantages unattainable with traditional materials. By grounding material innovation in both environmental responsibility and practical performance, this study seeks to offer a viable pathway toward a more resilient, sustainable, and resource efficient food packaging.

Table 1
Comparative overview of PLA/PHB blends plasticized with different bio-based additives and their main properties.

Ref.	Blend Composition	Additive Concentrations	Main improvement	Remarks
Armentano et al. (2015) [11]	PLA/PHB (85:15)	Oligomeric lactic acid (OLA) (15–30 wt%)	Improved ductility, lower Tg, improved WVTR, enhanced compatibility	Increased oxygen permeability at high OLA contents
Aimilia et al. (2024) [12]	PLA/PHB (75:25)	Epoxidized soybean oil methyl ester (ESOME) (5–10 wt%)	Improved flexibility, toughness, oxygen barrier properties, and processability	Migration remained acceptable up to 7.5 wt%; focused mainly on packaging performance
Abdelwahab et al. (2012) [13]	PLA/PHB (75:25)	Polyester plasticizer (Lapol 108) (5–7 wt%)	Improved elongation at break, miscibility, and thermal behavior; decreased Tg	Limited biodegradation improvement; no functional barrier or antioxidant properties reported
Arrieta et al. (2014) [14]	PLA/PHB (75:25)	Poly(ethylene glycol) (PEG) and acetyl tributyl citrate (ATBC) (15 wt%)	Improved flexibility, oxygen barrier, transparency, and thermal stability	ATBC showed superior compatibility and plasticization efficiency; no antioxidant functionality reported
Sempere-Torregrosa et al. (2022) [15]	PLA/PHB (75:25)	Epoxidized corn oil (ECO) and maleinized corn oil (MCO) (1–10 wt%)	Improved ductility, impact resistance, and compatibilization; decreased Tg	Mechanical strength decreased and cavitation observed at high oil contents; barrier and antioxidant properties were not evaluated

2. Materials and methods

2.1. Materials

2.1.1. Polymers

Poly(lactic acid) (PLA, Biopolymer 2003D, commercial grade) was provided in pellet form by NatureWorks LLC (Minnetonka, MN, USA), with a density of 1.24 g cm^{-3}. A PLA–PHB blend containing 25 wt% PHB (commercial grade P226E) was supplied in pellet form by Biomer (Krailling, Germany), showing a density of 1.25 g cm^{-3}.

2.1.2. Vegetable oil

Food-grade corn oil (CO) was used as the vegetable oil feedstock for the subsequent epoxidation and maleinization reactions. The chemical modification of the oil was monitored through the evolution of oxirane oxygen content during epoxidation and acid number variation during maleinization, according to the corresponding standardized methodologies.

The progress of the epoxidation reaction was evaluated according to ASTM D1652-97 and ISO 3961:2009 standards through oxirane oxygen determination. Similarly, the maleinization process was monitored through acid number evolution, confirming the successful incorporation of functional groups into the vegetable oil structure. The maleinization ratio (4–8 wt% maleic anhydride grafting) and the apparent molecular weight increase (1000–1600 g/mol) reported for the modified oils are taken from values commonly reported in the literature for corn oil-based epoxidized and maleinized systems with comparable conversion levels. These values are provided to support a realistic description of the chemical modification and to aid comparison with previously reported systems.

2.2. Film extrusion

The processing workflow illustrated in Fig. 1 outlines a controlled hot melt extrusion strategy that shaped the final performance of the polymeric films through a sequential two stage manufacturing route. Initially, all PLA based materials including the formulations containing specific weight percentages of Eo and Mo underwent a standardized preparation protocol. The concentration of compatibilizer/plasticizer agents was selected according to previous preliminary study, in which different loading levels were evaluated in PLA–PHB systems. The selected contents (2.5 and 10 wt%) were identified as suitable concentrations to achieve effective modification of the polymer matrix while maintaining adequate processability and structural integrity. Lower concentrations showed limited effects on the blend properties, whereas higher contents promoted excessive plasticization and deterioration of the mechanical performance [15]. PLA pellets from the same batch were first dried for 12 h at 40 °C in an MDEO dehumidifier oven (Industrial Marsé, Barcelona, Spain) to minimize moisture induced degradation during melt processing. The dried pellets were then premixed with the designated amounts of vegetable oils through mechanical stirring for 5 min, ensuring an initial macroscale dispersion of the additives prior to melting compounding.

To achieve full homogenization, the premixed materials were processed in a co-rotating twin screw extruder (Dupra SL, Alicante, Spain; L/D = 24). The temperature profile from hopper to die was set at 110, 115, 120, and 125 °C, with a screw speed of 20 rpm, enabling controlled shear conditions suitable for both PLA melting and oil incorporation. This step yielded compounded materials exhibiting uniform morphology and compositional consistency, a necessary prerequisite for stable film formation. After extrusion, the strands were air cooled for 30 min and mechanically pelletized using an ALBI-TECH MME-01 multifunctional grinding unit (Chelm, Poland) to obtain granules with reproducible geometry for downstream processing.

In the second stage, the compounded pellets were transformed into films through blown film extrusion using a Microex system (Eurotech Extrusion Machinery Srl, Tradate, Italy). The temperature settings were adjusted to 125, 130, 130, and 125 °C from feed to die, maintaining a constant 20 rpm screw speed to ensure gentle yet effective remelting of the modified PLA blend. The polymer melt was then extruded through a circular die to form a tubular flow, which was inflated by a calibrated air stream to generate a stable bubble. Real time regulation of bubble diameter and film gauge was achieved through the coordinated action of the air ring, collapsing frame, and nip roller assembly. The thickness of the developed films varied between 40 and 100 μm, which was influenced by the formulation composition and the processing conditions during extrusion and film formation.

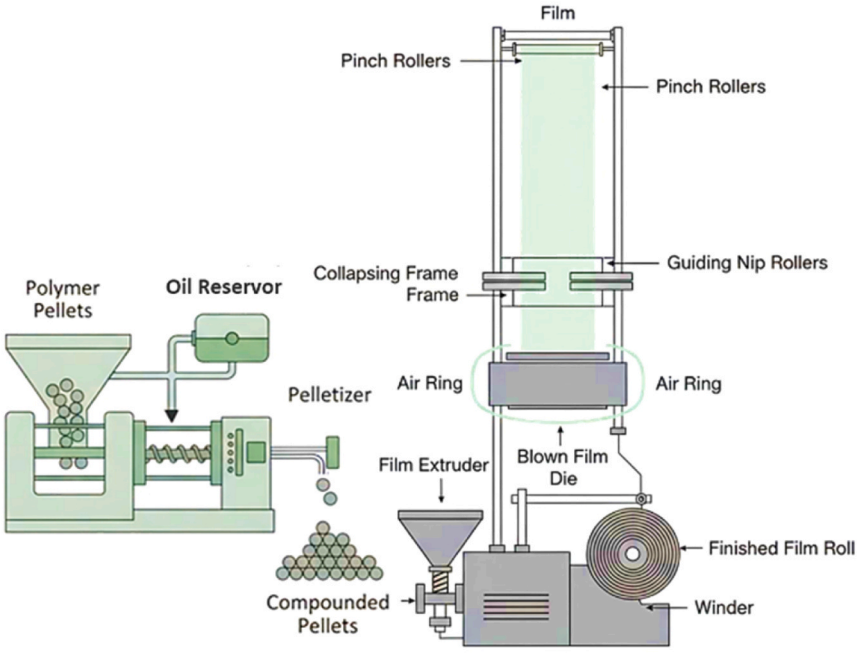

Fig. 1. Flowchart for obtaining the film.

2.3. FTIR-ATR spectra

The molecular interactions between the vegetable oils and the biopolymer blend were probed using a Perkin-Elmer BX FTIR/ATR infrared spectrometer (Madrid, Spain), enabling a detailed evaluation of potential chemical affinities, compatibilization effects, and structural rearrangements induced by the additives. Spectra were collected in the 4000–400 cm^{-1} wavenumber region at a resolution of 4 cm^{-1}, averaging 11 scans to improve the signal to noise ratio and ensure robust peak definition. Subsequent spectral processing and baseline refinement were performed using the Prestige IR Solution software, allowing for the accurate interpretation of functional group variations associated with polymer-oil interactions.

To complement the spectroscopic insights, the microstructural organization of the films was examined by high resolution field-emission scanning electron microscopy (HR-FESEM) using an AURIGA Zeiss platform (JEOL JSM-7000F, Zeiss, Kyoto, Japan). This analysis provided nanoscale visualization of surface morphology, revealing phase distribution, dispersion quality, and microstructural features directly correlated with the chemical modifications identified through FTIR.

2.4. Thermal analysis

Thermal stability was evaluated by thermogravimetric analysis (TGA) using a TGA PT1000 analyzer (Linseis Inc., Selb, Germany). Samples with masses ranging from 15 to 20 mg were subjected to a heating program from 30 °C to 700 °C at a rate of 10 °C min^{-1} under a nitrogen atmosphere maintained at a flow rate of 30 mL min^{-1}.

The miscibility of the materials was evaluated by analysing their thermal properties using differential scanning calorimetry (DSC). The thermoanalytical tests were carried out using a Discovery DSC 25 equipment from TA Instruments (New Castle, DE, USA). The sample weight range was 5–10 mg. An equilibration step to 25 °C for 1 min was set, followed by an initial heating program from 25 to 180 °C to remove thermal history, then a cooling program from 180 to −50 °C, and finally a second heating program from −50 to 250 °C, all performed at a constant rate of 10 °C min^{-1} under a nitrogen atmosphere with a flow rate of 66 mL min^{-1}. Using this technique, the glass transition temperature (Tg), cold crystallization peak (Tcc), and melt peak temperature (Tm) of the control PLA and the PLA blend formulations were identified. The degree of crystallization (Xc) was calculated using Eq. (1).

To enable direct comparison between samples, the heat flow data were normalized to each sample's initial mass and reported as specific heat flow in watts per gram (W/g). This normalization was performed using the TA Instruments TRIOS software by dividing the absolute heat flow (mW) by the sample's exact mass (mg). By convention, exothermic transitions are displayed pointing upwards in the thermograms.

$$X_C(\%) = 100 * \frac{|\Delta H_{CC} + \Delta H_m|}{\Delta H_m(100\%)} * \frac{1}{W_{PLA}} \quad (1)$$

Where ΔH_{CC} is the cold crystallization enthalpy, ΔH_m is the melt enthalpy, ΔH_m (100%) is the theoretical melt enthalpy for a fully crystalline PLA structure (93 J g^{-1}), and WPLA is the PLA weight fraction

2.5. Optical analysis

The optical behavior of films was evaluated through UV–Vis spectroscopic analysis using a Cary 100 UV–Vis spectrophotometer (Agilent Technologies, Barcelona, Spain). Spectra were collected across the 190–700 nm wavelength range, enabling a comprehensive assessment of light transmission in both the ultraviolet and visible domains. This approach provided quantitative insights into the films' optical clarity and phase homogeneity, properties directly influenced by additive incorporation and polymer oil interactions.

2.6. Contact angle

Surface wettability was quantified through static water contact angle measurements performed at room temperature using the sessile drop technique on an Easy Drop Standard goniometer FM140 (KRÜSS GmbH, Hamburg, Germany), equipped with a stroboscopic imaging system and Drop Shape Analysis software (SW21; DSA1). Distilled water was dispensed onto the film surface using a precision microsyringe, generating droplets ranging from 2 to 6 μL. Following deposition, the droplet was allowed to equilibrate for approximately 60 s prior to the initial measurement, after which four additional readings were acquired at 10 s intervals to capture any time dependent relaxation of the surface. All measurements were performed in triplicate at randomly selected positions on each film, ensuring statistical robustness and minimizing local morphological bias.

2.7. Mechanical characterization

Tensile performance was assessed using an ELIB 50 universal testing machine (S.A.E. Ibertest, Madrid, Spain), operating at ambient laboratory conditions and equipped with a 5 kN load cell to ensure high fidelity force measurements. Mechanical testing was conducted according to the ISO 527 guidelines, with films precisely cut into standardized specimens measuring 10 mm in width and a gauge length of 100 mm. Each strip was elongated at a constant crosshead speed of 10 mm min^{-1}, allowing reliable characterization of the elastic–plastic response of the materials. To ensure statistical robustness, a minimum of five independent replicates was analyzed for each formulation, generating a dataset capable of capturing intrinsic variability associated with processing induced microstructural differences.

2.8. Water vapor transmission rate

The water vapor barrier performance was assessed through water vapor transmission rate (WVTR) measurements following ASTM E96/E96M (desiccant method). Circular film samples, with a diameter of 63.75 mm, were sealed over permeation cells containing 2 mg of silica gel per sample and placed in a controlled humidity chamber maintained at 23 °C and 90% RH. Periodic mass changes of each cell were recorded in the 8 initial hours and 24 h after the test began using an analytical balance, and WVTR values were determined from the steady state region of the mass gain curve. Tests were conducted in triplicate to ensure reproducibility.

2.9. Food contact test

Fresh persimmons originating from the same production lot and grown under identical agronomic conditions were selected to assess the capacity of the developed films to delay quality degradation driven by oxidative browning and fungal proliferation. To ensure uniform and intimate contact with the packaging material, each persimmon was sliced, and the films were applied directly onto the exposed pulp surface. The progression of discoloration, tissue softening, and mold development was monitored over a 15 days storage period at room temperature, without the use of controlled atmospheres such as vacuum sealing or inert gas flushing.

3. Results

3.1. Film formulation

The hot extrusion process enabled the fabrication of four bioplastic film formulations, A, B, C, and D, whose precise compositional profiles are shown in Table 1. Formulation A, composed of 100% PLA by weight, produced films with a highly uniform appearance, reflecting the predictable melt behavior and structural consistency typical of pure PLA.

The introduction of 25% PHB by weight into formulation B significantly altered the film's microstructure, resulting in a stiffer material. These changes are consistent with the known tendency of PHB to enhance structural order within PLA-based matrices, thus influencing melting elasticity and solid state morphology.

Formulations C and D produced films with significantly improved process stability compared to formulation B. The presence of Mo or Eo acted as an effective compatibilizing component, facilitating more consistent mixing between PLA and PHB and reducing phase discontinuities during extrusion. This synergistic effect produced films with smoother surface characteristics and greater structural uniformity [15] (Table 2).

3.2. Chemical interaction

The FTIR spectra presented in Fig. 2 reveal a clear evolution of the chemical structure across samples A–D, reflecting the progressive incorporation of functionalized vegetable oil derivatives into the PLA/PHB polymer blend.

Sample A exhibits the canonical vibrational features of aliphatic polyesters, including the strong and sharp ester carbonyl stretching band at ~1758–1762 cm^{-1}, which is associated with the C═O groups of the lactide repeating units [15,16]. The C–H stretching region between 2995 and 2945 cm^{-1} shows well defined asymmetric and symmetric vibrations of –CH_3 groups, while the bands at ~1455 and ~1380 cm^{-1} correspond to CH_3 bending and deformation modes. The fingerprint region is dominated by intense C–O–C stretching vibrations at ~1180, 1125, and 1080 cm^{-1}, along with weaker contributions near ~1045 cm^{-1}, reflecting the ordered ester backbone of PLA.

B retains all major PLA related absorptions but displays subtle spectral rearrangements. The carbonyl band slightly broadens and shifts toward lower wavenumbers, indicating the superposition of PHB ester carbonyl vibrations, typically located around ~1725–1740 cm^{-1}. Additionally, increased intensity in the C–H stretching region (2970–2930 cm^{-1}) and in the CH_2 bending bands at ~1460 cm^{-1} reflects the higher methylene content of PHB [17]. These changes suggest enhanced dipole-dipole interactions and partial disruption of PLA chain packing, while still indicating a predominantly physical blend without new covalent linkages.

The incorporation of 2,5 wt% maleinized corn oil, sample C, leads to more pronounced and systematic spectral modifications. The carbonyl region becomes significantly broader and asymmetric, extending from ~1780 to ~1700 cm^{-1}, consistent with overlapping contributions from PLA/PHB ester groups and the anhydride or maleate derived carbonyl functionalities introduced by Mo, an effect linked to enhanced interfacial interactions reported for functionalized oil additives [18]. The aliphatic C–H stretching bands at ~2925 and ~2855 cm^{-1} intensify, confirming the incorporation of long triglyceride chains. In the 1250–1000 cm^{-1} region, increased absorbance and peak merging indicate enrichment in oxygenated groups and modification of the local polymer environment. Furthermore, subtle changes in the 950–850 cm^{-1} range may be associated with maleinized moieties interacting with the polyester backbone.

Sample D exhibits the most extensive spectral evolution. The aliphatic C–H stretching region (2950–2850 cm^{-1}) shows a marked intensity increase, reflecting the high content of saturated hydrocarbon chains from Eo. Notably, modifications in the 1250–1000 cm^{-1} domain become more pronounced, with band reshaping near ~1160 and ~1030 cm^{-1}, consistent with contributions from epoxy related C–O stretching vibrations [19]. Although the characteristic oxirane ring absorption near ~820–850 cm^{-1} is partially overlapped by the polymer fingerprint region, its attenuation and broadening suggest partial epoxy ring opening and interaction with ester or hydroxyl groups of PLA and PHB during extrusion. The carbonyl band remains broad and less symmetric than in samples A and B, supporting the presence of strong local interactions and altered chain packing.

Table 2
Composition of the prepared PLA–PHB formulations.

Label	Material Composition			
	PLA (wt%)	PHB (wt%)	Eo (wt%)	Mo (wt%)
A	100	---	---	---
B	75	25	---	---
C	73,75	23,75	---	2,5
D	70	20	10	---

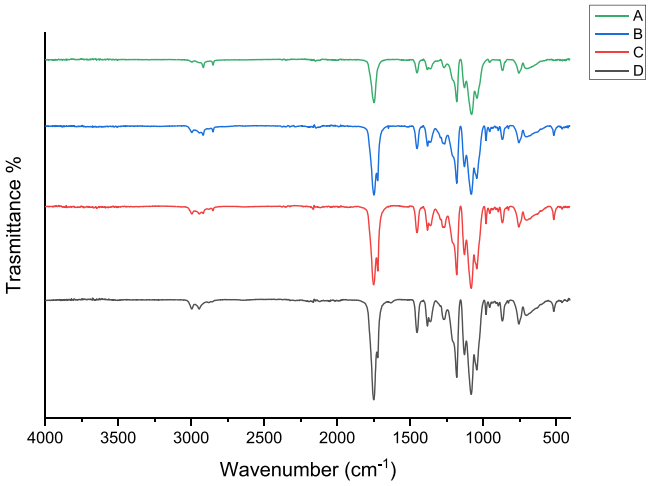

Fig. 2. FTIR-ATR spectra of samples A–D showing the evolution of the vibrational profile upon incorporation of epoxidized corn oil (Eo) and maleinized corn oil (Mo) into the PLA/PHB blend.

3.3. Thermal characterization

The thermogravimetric analysis (TGA) curves of the developed formulations are presented in Fig. 3, while the corresponding thermal degradation parameters are summarized in Table 3. All materials exhibited a main degradation stage between approximately 250 and 380 °C, which is characteristic of PLA- and PHB-based systems.

Neat PLA showed the highest initial thermal stability among all formulations, with a $T_{5\%}$ value of 311.3 °C. The degradation process occurred in temperature range, indicate the typical thermal decomposition behavior of PLA. After blending PLA with PHB, the initial thermal ($T_{5\%}$) stability decreased considerably, to 286.4 °C. This behavior can be

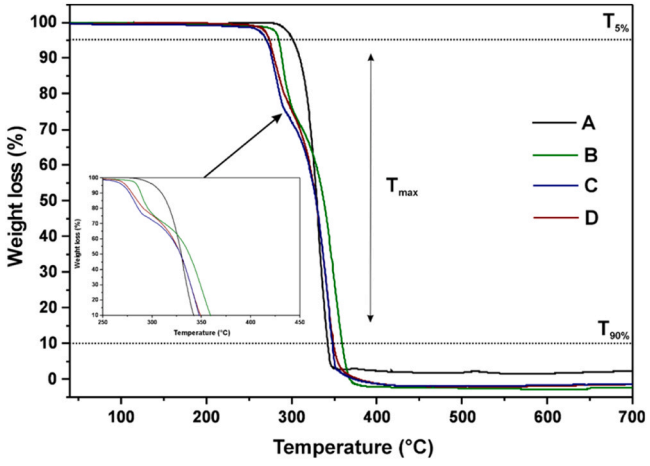

Fig. 3. Thermogravimetric analysis (TGA) curves of samples A–D showing the thermal degradation behavior and characteristic decomposition temperatures.

Table 3
Thermal properties of samples A–D obtained from TGA and DSC analyses.

Code	TGA Parameters			DSC Parameters						
	$T_{5\%}$ (°C)	T_{max} (°C)	$T_{90\%}$ (°C)	T_g (°C)	T_{cc} (°C)	ΔH_{cc} (J/g)	T_{mPLA} (°C)	ΔH_m (J/g)	X_c (%)	T_{mPHB} (°C)
A	311.3	330.5	342.6	58.10	110.92	24.83	150.37	25.24	0.45	-
B	286.4	349.1	359.4	48.00	123.82	16.90	148.67	12.70	0.00*	165.00
C	270.1	329.2	348.0	44.18	115.25	16.01	151.6	6.33	0.00*	168.28
D	270.9	328.7	338.7	49.55	125.61	4.9	150.4	3.15	0.00*	170.27

* Mathematical calculation yielded negative values due to ΔHcc > ΔHm, indicating an initially fully amorphous PLA phase (Xc ≈ 0%).

attributed to the lower thermal stability of PHB, which is more susceptible to thermal degradation. Nevertheless, the PLA–PHB blend exhibited the highest T_{max} value (349.1 °C), suggesting that although the degradation process started earlier, the maximum degradation rate occurred at higher temperatures compared to neat PLA.

The incorporation of maleinized corn oil (Mo) and epoxidized corn oil (Eo) reduced the initial thermal stability of the blends. The formulations PLA–PHB–2.5 wt% Mo and PLA–PHB–10 wt% Eo presented similar $T_{5\%}$ values of 270.1 and 270.9 °C, respectively. This reduction is associated with the plasticizing effect of the modified oils, which increased polymer chain mobility and facilitated thermal degradation at lower temperatures. In addition, the presence of reactive functional groups in the modified oils may also contribute to the earlier onset of degradation.

Despite the decrease in the initial degradation temperatures, all plasticized systems maintained relatively high thermal stability, with degradation occurring well above conventional processing temperatures used for PLA- and PHB-based materials. Regarding the final degradation stage, the Eo-plasticized formulation showed the lowest $T_{90\%}$ value, indicating a faster and more complete degradation process at high temperatures. This behavior may be related to the enhanced molecular mobility induced by the epoxidized oil and the lower thermal resistance of the more flexible polymer network.

TGA results demonstrated that the incorporation of PHB and modified vegetable oils affected the thermal degradation behavior of PLA-based blends, mainly by reducing the onset degradation temperatures due to increased chain mobility and the lower thermal stability of the added components. However, all developed formulations preserved sufficient thermal stability for conventional melt-processing applications.

The thermal transitions of samples A–D were investigated by differential scanning calorimetry, and the corresponding thermograms are shown in Fig. 4 and Table 3. The neat PLA (Sample A) exhibited very low crystallinity (Xc = 0.44%), indicating a high amorphous nature under the processing conditions. Interestingly, for the PLA/PHB blends (Samples B–D), the mathematical evaluation of Eq. (1) resulted in negative values. Thermodynamically, this phenomenon occurs when the cold crystallization enthalpy (ΔHcc) exceeds the melting enthalpy (ΔHm). In polymer physics, this indicates that the PLA matrix was completely amorphous prior to the DSC scan (Xc ≈ 0%), and the crystalline structures melted during the endothermic event were exclusively formed during the heating ramp.

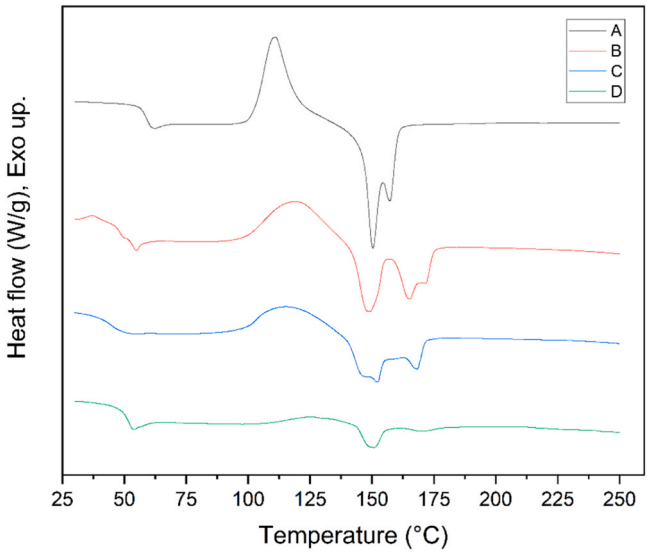

Fig. 4. Differential scanning calorimetry (DSC) curves of samples A–D showing the glass transition, cold crystallization, and melting behavior.

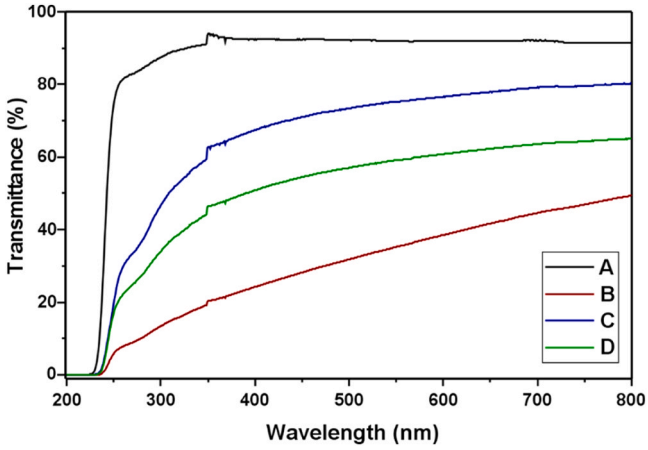

Fig. 5. UV–Vis transmittance spectra of samples A–D, highlighting the influence of epoxidized corn oil (Eo) and maleinized corn oil (Mo) on the optical behavior of PLA/PHB-based films.

3.4. Optical properties

The optical characterization reported in Figs. 5 and 6 provides a comprehensive assessment of how the incorporation of functionalized vegetable oils modulates the transparency and light transmission behavior of the PLA/PHB-based materials. The UV-Vis transmittance curves (Fig. 5) reveal a clear differentiation among the four formulations (A–D). Sample A exhibits the lowest transmittance across the entire measured spectrum, indicating a more heterogeneous microstructure and higher intrinsic opacity [20]. In contrast, the samples containing modified oils, particularly formulations C and D, exhibit a marked increase in transmittance, reflecting an enhanced homogeneity of the polymer blend and improved dispersion of phases.

The steep rise in transmittance observed in samples C and D at lower wavelengths suggests that the epoxidized and maleinized corn oils promote a reduction in light scattering centers, likely due to their compatibilizing action at the PLA/PHB interface. The smoother progression of the transmittance curve for sample D is especially noteworthy, as it indicates a more efficient refractive index matching between the polymeric phases, a typical consequence of reduced phase

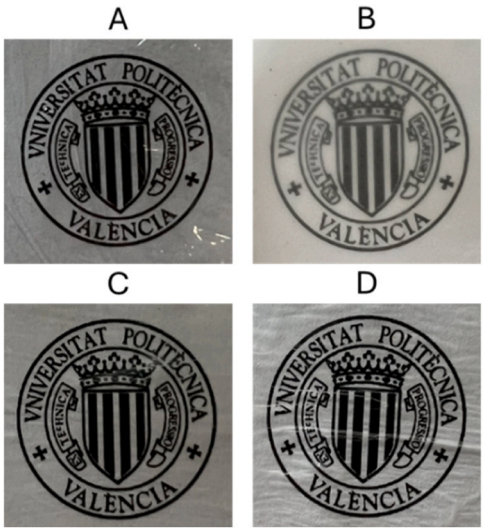

Fig. 6. Visual transparency of samples A–D assessed by placing the films over a high contrast printed logo of the Polytechnic University of Valencia.

separation and improved interfacial adhesion. Sample B exhibits intermediate optical behavior, confirming that the partial incorporation of the modified oils results in measurable optical improvements.

These spectroscopic trends are further corroborated by the visual clarity assessment shown in Fig. 6. When positioned over a high contrast printed logo, the films exhibit differences that align with the UV–Vis measurements. Sample A appears noticeably hazier, with diffuse transmission that blurs the fine details of the underlying image. The edges of the emblem are less defined, confirming the greater internal scattering expected from a less compatible and more phase segregated polymer blend. Sample B offers a slight improvement, but residual opacity remains evident.

In contrast, samples C and D provide significantly sharper image reproduction, with enhanced contour definition and more uniform light transmission. Sample D demonstrates excellent visual clarity, preserving even the small typographic features of the logo. This enhanced transparency can be attributed to the dual role of epoxidized and maleinized oils: their plasticizing effect reduces microdefects and density fluctuations, while their compatibilizing function mitigates interfacial discontinuities that would otherwise contribute to scattering.

Taken together, the UV–Vis transmittance profiles and qualitative optical images demonstrate that the incorporation of chemically modified corn oils not only influences the mechanical and interfacial properties of the PLA/PHB blends, but also markedly improves their optical performance. This synergy between molecular level compatibilization and macroscopic transparency highlights the potential of such bio-derived additives to generate biopolymer films suitable for applications requiring controlled visibility, aesthetic quality, or optical monitoring of food freshness.

3.5. Static water contact angle

The first insight into the interfacial behavior of the developed bioplastics emerges from their surface wettability, as presented in Fig. 7(b) and visually corroborated by the droplet profiles in Fig. 7(a). Contact angle measurements reveal how the chemical architecture introduced through PHB blending and oil functionalization governs the interaction between the material surface and aqueous media, an attribute of direct relevance for food packaging, where moisture management strongly influences both microbial stability and textural preservation of fresh produce [21].

Neat PLA (A) exhibits a moderately hydrophobic surface, with a contact angle of approximately 79°, reflecting its intrinsically low

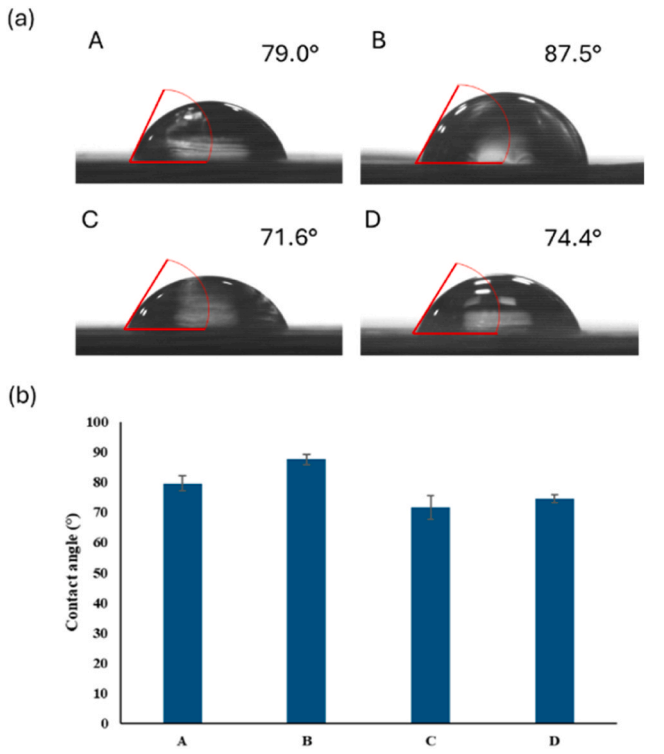

Fig. 7. Representative droplet profiles used for contact-angle determination of materials A–D (a) and static water contact angles of the four material formulations A–D (b).

surface polarity. Upon blending PLA with PHB (B), the surface becomes markedly more hydrophobic, reaching the highest contact angle in the series (~87,5°). This increase suggests that PHB not only contributes to its well known barrier forming characteristics but also rearranges the near surface morphology of the blend, reducing polar segment exposure and enhancing water repellent behavior.

A contrasting trend emerges upon incorporation of the functionalized vegetable oils. The addition of 2,5 wt% maleinized corn oil (C) leads to a significant reduction in the contact angle (~71,6°), indicating a transition toward higher wettability. This effect is consistent with the presence of epoxide rings, which introduce polar functionalities that increase water affinity at the interface. Meanwhile, the formulation containing 10 wt% epoxidized corn oil (D) exhibits a slightly higher but still reduced contact angle (~74,4°) compared to neat PLA. The maleinized groups likewise contribute additional polar sites, although at higher oil content, partial surface plasticization may induce chain mobility and dynamic rearrangements that moderate the overall increase in hydrophilicity. The incorporation of both modified oils increases the surface polarity of the films, promoting stronger interactions with water molecules at the interface. Furthermore, the higher oil content may enhance chain mobility and surface rearrangement phenomena, contributing to the observed variations in wettability behavior.

3.6. Mechanical properties

The mechanical characterization of the four material blends (Fig. 8) reveals how PHB incorporation and bio-based oil functionalization reshape the balance between stiffness, strength, and ductility within the PLA matrix. Neat PLA (A) exhibits the typical behavior of a brittle biopolymer, combining relatively high tensile strength with limited elongation at break and a rigid modulus. This baseline response reflects the intrinsic characteristics of PLA, whose restricted chain mobility and semicrystalline morphology limit plastic deformation and fracture resistance.

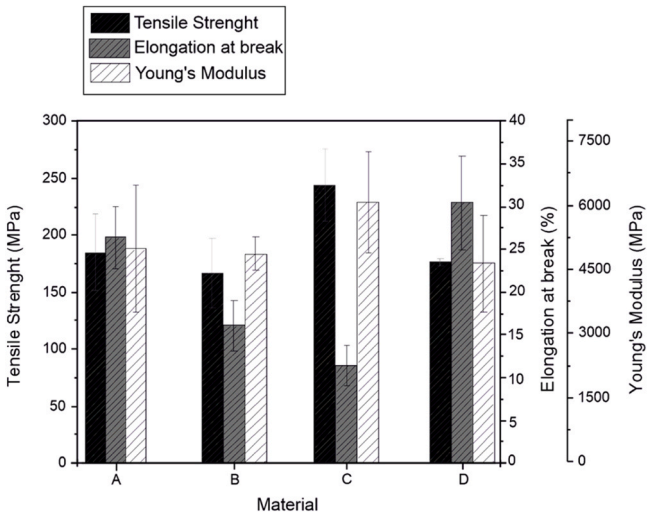

Fig. 8. Mechanical properties of materials A–D. The figure compares tensile strength, elongation at break, and Young's modulus, showing the strengthening effect of epoxidized corn oil and the improved ductility provided by maleinized corn oil.

The PLA/PHB blend (B) exhibits a moderate decrease in tensile strength compared to neat PLA, consistent with the limited miscibility and morphological heterogeneity commonly observed in PLA/PHB systems. Despite this reduction, the Young's modulus remains essentially comparable, indicating that PHB incorporation does not significantly compromise the overall stiffness of the material. In contrast to the previous interpretation, the elongation at break of formulation B decreases relative to neat PLA, indicating a further reduction in ductility. This behavior is consistent with the presence of phase-separated domains and interfacial defects that act as stress concentration points, promoting earlier crack initiation and failure under tensile loading.

A more pronounced transformation is observed upon adding 2,5 wt% maleinized corn oil (C). This formulation displays the highest tensile strength among all samples, accompanied by a substantial increase in Young's modulus. Such simultaneous reinforcement in strength and stiffness is indicative of successful reactive compatibilization, where the epoxide groups are likely to promote interfacial bonding between PLA and PHB, thereby reducing phase separation and creating a more coherent load transfer network [22]. However, elongation at break is significantly reduced, implying that the improved structural integrity is achieved at the expense of ductility, resulting in stiffer and stronger but less extensible material.

Conversely, the introduction of 10 wt% epoxidized corn oil (D) yields a more balanced mechanical response. Tensile strength and modulus remain high, only slightly below those of material C, while elongation at break increases markedly. This indicates that maleinized corn oil acts predominantly as a reactive plasticizer compatibilizer, enhancing interfacial adhesion while simultaneously promoting segmental mobility. The resulting formulation integrates structural robustness with improved deformability, offering a promising compromise between strength and toughness.

3.7. Water vapor transmission rate

As shown in Fig. 9, the different formulations exhibit distinct moisture-barrier responses. Neat PLA (A) presents the highest sensitivity to water vapor, reflected by the steepest increase in mass variation over time. This behavior aligns with its well-known limitations in resisting moisture permeation, especially in applications exposed to humid environments.

The introduction of PHB in the PLA/PHB blend (B) significantly reduces the rate of moisture transfer, as evidenced by the lower slope

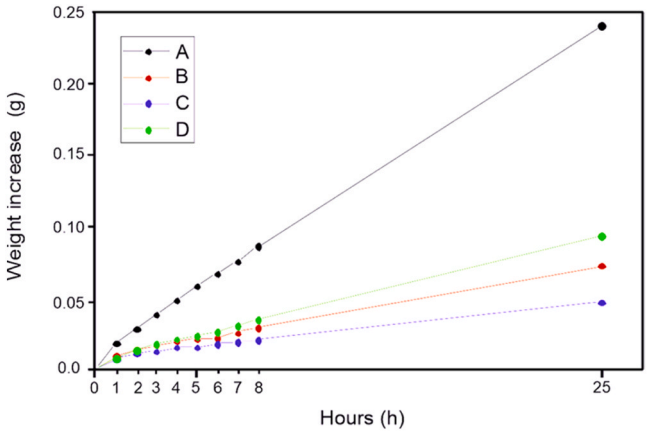

Fig. 9. Weight gain over time of PLA, PLA/PHB, and oil modified PLA/PHB blends.

compared with neat PLA. This improvement is attributed to PHB's higher crystallinity and inherently superior barrier performance, which restricts molecular diffusion through the blend. A further improvement is observed in Material C, containing 2,5 wt% maleinized corn oil, which exhibits an additional decrease in moisture transfer. The improved barrier response suggests that enhanced interfacial adhesion is promoted by the functionalized oil, resulting in a more compact morphology with fewer diffusion pathways. This reduction suggests that epoxide polymer interactions enhance interfacial adhesion, creating a more compact morphology that hinders diffusion pathways.

Material D, functionalized with 10 wt% epoxidized corn oil, shows the lowest moisture related mass variation across the entire measurement period. This behavior indicates the formation of a dense and cohesive network, in which the reactive groups of the oil promote compatibilization while controlling chain mobility, thereby further restricting vapor transport. Its minimal mass increase over time indicates a dense and cohesive network in which maleinized groups promote reactive compatibilization while also imparting controlled plasticization. The resulting structure restricts water ingress more effectively than the other formulations.

These trends are quantitatively confirmed in the water vapor transmission rate (WVTR) data presented in Fig. 10. Neat PLA (A) exhibits the highest WVTR, while the PLA/PHB blend (B) shows a substantial decrease, consistent with PHB's superior barrier properties. Materials C and D achieve further reductions, with D reaching the lowest WVTR value of the series. These results demonstrate that functionalized vegetable oils, especially maleinized corn oil, significantly enhance moisture barrier performance by reinforcing interfacial compatibility and reducing microstructural defects. This reduction occurs despite the

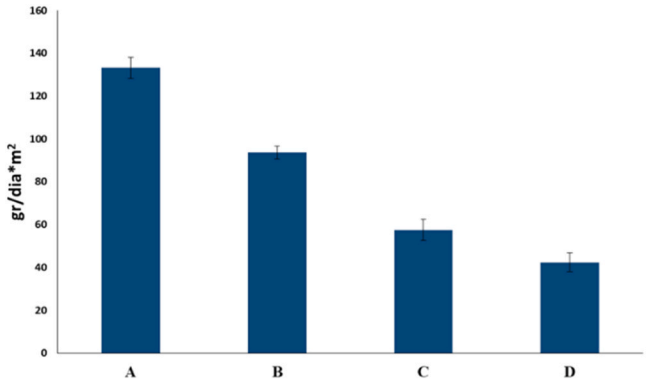

Fig. 10. Reduction of water vapor transmission rates in PLA/PHB blend rough epoxidized and maleinized corn oil functionalization.

potential increase in chain mobility typically associated with oil based plasticizers. In functionalized oils, reactive groups promote stronger interfacial interactions, helping to fill microvoids within the blend and leading to a more cohesive and compact structure. As a result, the domain effect is morphological densification rather than plasticization, effectively limiting vapor diffusion through the material.

Therefore, although the modified formulations exhibited slightly higher surface wettability, the WVTR results suggest that moisture transport was predominantly governed by the bulk structure of the films rather than by surface interactions alone. This behavior may be associated with improved phase compatibility and a reduction of preferential diffusion pathways within the polymer matrix. However, free volume and diffusion pathway modifications were not directly quantified in the present study and are proposed based on the overall morphological and barrier performance observations.

3.8. Food contact analysis

The outcomes of the food contact test conducted on sliced persimmon after 15 days of storage at room temperature (Fig. 11) clearly demonstrate the influence of the different bioplastics films on fruit preservation. The unwrapped control exhibits rapid and severe deterioration, characterized by an extensive darkening of the pulp, tissue collapse, and visible fungal contamination, which are hallmarks of uncontrolled moisture loss and microbial proliferation in highly perishable fruits [23,24].

In contrast, all packaged samples show delayed degradation relative to the control, yet the extent of preservation varies markedly with film composition. Persimmons wrapped in neat PLA (A) display moderate dehydration and browning, indicating partial moisture retention but insufficient breathability to prevent textural collapse and localized spoilage.

The PLA/PHB blend (B) offers improved performance: the fruit maintains greater structural integrity and shows reduced browning, suggesting that the blend's enhanced barrier properties help moderate water exchange while slowing microbial development.

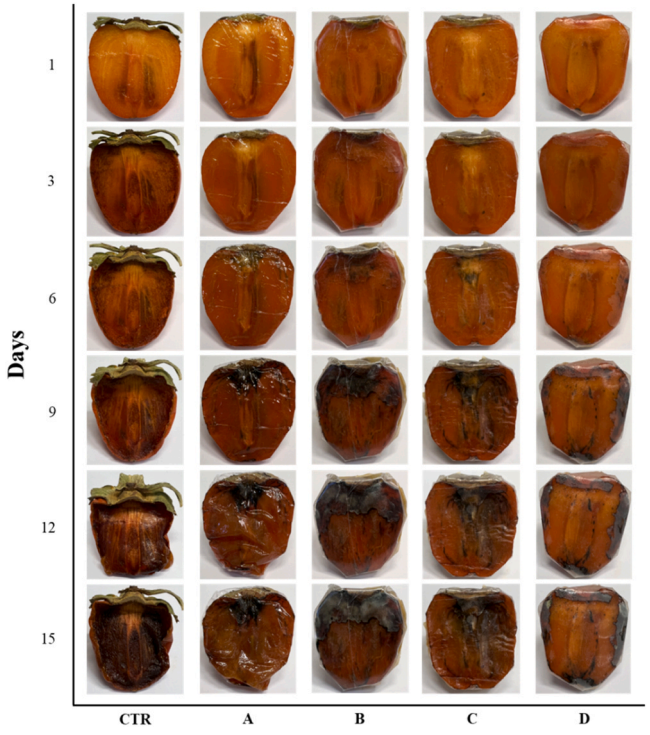

Fig. 11. Food contact test on sliced persimmon after 15 days of storage with and without the bioplastic film stored at room temperature.

A more pronounced protective effect is observed in the samples wrapped with PLA/PHB containing 2,5 wt% maleinized corn oil (C). These fruits retain a firmer texture and exhibit visibly lower fungal growth, with the slices showing fewer darkened zones compared to A and B. The improved outcome aligns with the film's intermediate moisture buffering capacity, which likely helps stabilize the fruit microenvironment.

The most significant preservation is achieved with PLA/PHB functionalized with 10 wt% epoxidized corn oil (D). The persimmon slices wrapped in this material exhibit the least browning and minimal microbial proliferation, maintaining a more natural color and overall structural cohesion even after 15 days. This behavior suggests that the D film provides an optimized balance between barrier performance and controlled permeability, limiting excessive moisture accumulation while preventing dehydration induced tissue stress.

4. Discussion

4.1. Structure–property relationships and molecular interactions

The results across all analytical domains collectively reveal a coherent and highly interdependent relationship between structure, properties, and functionality within the modified PLA/PHB blend demonstrating how compositional tuning drives molecular reorganization, morphological refinement, and optimal performance in practical food packaging scenarios. The progressive transition from neat PLA (A) to increasingly complex formulations (B–D), whose detailed compositions are reported in Table 1, demonstrates that the melt extrusion process not only accommodates but actively amplifies the chemical interactions induced by PHB and modified oils, enabling the emergence of distinct structural regimes that govern the materials' optical, mechanical, and barrier behavior [25]. The uniformity of formulation A reflects the predictable melt behavior of pure PLA.

However, its performance also exposes intrinsic limitations, including heterogeneous microtextures, lower optical transmittance, higher weight over time, and faster degradation of packaged produce [26]. The introduction of 2,5 wt% PHB in formulation B immediately disrupts this scenario by increasing stiffness and hydrophobicity while reducing transparency, confirming that PLA/PHB immiscibility generates interfacial discontinuities that can be traced throughout all subsequent analyses [27]. The FTIR spectra support this interpretation by revealing sharp, well defined polyester signals with minimal broadening in A and B, indicating limited chemical interplay between the two polymers.

However, the incorporation of maleinized (Mo) or epoxidized (Eo) corn oils in formulations C and D profoundly changes this landscape. Spectral broadening in the carbonyl region, intensified C–H stretching, and enriched C–O–C vibrational features confirm that both additives participate in molecular level interactions rather than remaining physically dispersed [28]. These interactions likely include partial epoxide ring opening, anhydride reactivity, and localized compatibilization effects that strengthen the interphase between PLA and PHB, thereby producing a more cohesive and chemically integrated blend [29]. This is consistent with the markedly improved processing stability of films C and D, both of which exhibit smoother bubble formation, fewer melt instabilities, and enhanced structural homogeneity during extrusion, indicating that interfacial tension is reduced and phase dispersion is significantly refined [30].

4.2. Optical, mechanical and barrier properties

These molecular reorganizations are reflected in optical behavior: the low transmittance and diffuse haze of formulations A and B contrast sharply with the high transmittance profiles of C and D. This demonstrates that functionalized oils effectively eliminate scattering centers typically caused by microvoids, interfacial gaps, and crystallinity

mismatches [31]. The unprecedented clarity of formulation D, both in UV–Vis spectra and visual imaging, suggests a nearly refractive index matched blends in which PLA-rich and PHB-rich domains have been minimized or smoothed at the nanoscale, a result rarely achieved in biopolyester blends without reactive compatibilizers [32]. Such optical refinement mirrors the mechanical transformations observed in tensile analysis. Neat PLA exhibits its characteristic brittleness, while the PLA/PHB film shows reduced tensile strength due to interfacial defects.

In striking contrast, formulation C achieves the highest strength and modulus, indicating that maleinized corn oil creates strong interfacial bonding and a rigid network that efficiently transfers stress across polymer domains [33]. Formulation D, on the other hand, achieves the most balanced profile, combining high strength and stiffness with significantly higher elongation at break. This reveals that epoxidized corn oil not only strengthens the interphase but also increases segmental mobility without compromising cohesion. This remarkable synergy suggests the formation of a molecularly entangled, partially plasticized yet structurally reinforced architecture capable of dissipating stress more efficiently than the unmodified material. These mechanical trends correlate strongly with water interaction behavior.

The contact angle results confirm that PLA/PHB (B) becomes more hydrophobic, likely due to PHB driven surface rearrangement, while the oil functionalized films become progressively more wettable, reflecting the migration or exposure of polar functionalities (epoxy, anhydride, hydroxyl) at the surface. WVTR data further reveal that, despite increased surface wettability, formulations C and especially D achieve superior barrier performance, with D showing the lowest weight over time and vapor transmission [34]. This apparent paradox suggests that plasticizers may promote a more cohesive bulk morphology, potentially reducing preferential diffusion pathways through the material. Therefore, while water molecules can interact more easily with the film surface due to the presence of polar functional groups, their transport through the bulk matrix may be hindered by improved phase compatibility and structural organization. However, free volume reduction and diffusion pathway modifications were not directly quantified in the present study and are proposed based on the combined interpretation of wettability and WVTR results.

The culmination of these interrelated structure property effects is evident in the food contact trials on sliced persimmon stored at room temperature for 15 days. The severe deterioration of the unwrapped control emphasizes the vulnerability of high moisture fruits to microbial proliferation and oxidative browning. PLA (A) confers only partial protection, consistent with its limited moisture buffering ability, while PLA/PHB (B) performs better due to its superior barrier properties. However, films C and, especially, D markedly extend fruit freshness. Formulation C delays browning and fungal development, while formulation D preserves structural integrity, color, and microbial stability to an extent far surpassing that of the other materials. This superior performance directly reflects formulation D's optimal balance of barrier regulation, interfacial compatibility, and controlled permeability, which together create a microenvironment that avoids both dehydration induced tissue collapses and moisture accumulation that would otherwise encourage microbial growth.

4.3. Industrial relevance and overall mechanistic interpretation

Despite the promising functional performance achieved by formulations C and D, some practical limitations related to the industrial scalability of PLA/PHB-based systems should also be considered. In particular, the relatively high cost of biodegradable polymers, especially PHB, remains one of the major constraints for the large-scale commercial implementation of these materials compared to conventional petroleum-based plastics. This economic challenge is widely recognized within the biopolymer sector and continues to limit the broader market penetration of fully biodegradable packaging solutions.

In the present study, the main objective was to improve the overall performance of PLA/PHB films through the incorporation of renewable corn-oil-derived additives acting as compatibilizers and plasticizers. From both sustainability and economic perspectives, the use of modified corn oil represents an attractive strategy because corn oil is an abundant, commercially available, and relatively low-cost agricultural resource compared to many specialized bio-based additives. Furthermore, the PHB content was intentionally limited to 25 wt% in order to balance enhanced material properties with reduced dependence on expensive biopolymer fractions.

Nevertheless, although the proposed formulations demonstrate clear improvements in transparency, mechanical behavior, barrier performance, and food preservation capability, the overall production cost is still expected to remain higher than that of conventional fossil-based packaging materials under current market conditions. At the same time, ongoing advances in industrial biotechnology, microbial fermentation processes, and large-scale biopolymer manufacturing are progressively contributing to the reduction of PHB production costs. Therefore, while the present formulations may still face economic limitations for immediate mass-market implementation, they represent a promising step toward the development of sustainable high performance packaging systems with enhanced functionality and reduced environmental impact.

When all results are considered holistically, a clear unifying mechanism emerges: functionalized vegetable oils, particularly epoxidized corn oil, act as molecular active compatibilizers that reorganize the PLA/PHB interface, reduce phase separation, refine morphology, enhance mechanical coherence, optimize water transport, and significantly extend food preservation performance. The transition from A to D thus represents a progression from a physically mixed system to a highly engineered, chemically integrated bioplastics whose properties emerge from synergistic interactions at multiple length scales. These findings highlight the transformative potential of bio-derived reactive additives in upgrading commercial biopolymers, positioning formulation D as a compelling candidate for next generation sustainable food packaging applications that require transparency, mechanical resilience, barrier efficiency, and demonstrated bio preservation capability.

5. Conclusions

The present study demonstrates that the structural, functional, and preservation performance of PLA-based materials can be profoundly enhanced through the synergistic incorporation of PHB and reactive, bio derived vegetable oils. The systematic comparison among the four formulations clearly shows that, while neat PLA and the PLA/PHB blend exhibit the intrinsic limitations of partially compatible biopolyesters, the addition of maleinized and especially epoxidized corn oil drives a fundamental reorganization of the polymer architecture, promoting interfacial compatibilization, morphological refinement, and controlled chain mobility. These molecular level modifications translate into macroscopic improvements, including superior optical clarity, increased mechanical strength and flexibility and optimized vapor barrier characteristics. Among all materials, the formulation containing epoxidized corn oil emerges as the most effective, achieving the best equilibrium between stiffness, ductility, and barrier behavior, and ultimately enabling the most significant extension of the shelf life of fresh cut persimmon under ambient storage. The integrated analysis of chemical, mechanical, barrier, and application level performances demonstrates that reactive plant derived oils represent a powerful strategy for engineering next generation biodegradable packaging films with properties tailored to real food preservation needs. Overall, this work provides a robust scientific basis for employing functionalized natural additives to overcome the inherent limitations of PLA/PHB blends, paving the way for scalable, sustainable, and high performance biopolymer packaging solutions.

CRediT authorship contribution statement

Federica Giuliano: Software, Methodology, Investigation, Formal analysis, Data curation. **María Dolores Samper:** Writing – review & editing, Writing – original draft, Visualization, Validation, Supervision, Funding acquisition. **Jaume Sempere-Torregrosa:** Software, Resources, Methodology, Investigation, Formal analysis. **Harrison de la Rosa-Ramírez:** Writing – original draft, Visualization, Supervision, Methodology. **Federico Barrino:** Writing – review & editing, Writing – original draft, Visualization, Validation, Supervision, Software, Methodology, Funding acquisition, Data curation, Conceptualization.

Declaration of Competing Interest

The authors declare that they have no known competing financial interests or personal relationships that could have appeared to influence the work reported in this paper.

Acknowledgements

This research was carried out by Dr. Barrino Federico, member of the European Union's Euratom Research and Training Programme (EURATOM) Horizon Europe, Grant no. 101061694.

H. de la Rosa-Ramírez thanks Universitat Politècnica de València for his post-doctoral Grant PAID-10-24.

Data availability

Data will be made available on request.

References

[1] B.L. Tardy, J.J. Richardson, L.G. Greca, J. Guo, J. Bras, O.J. Rojas, Advancing bio-based materials for sustainable solutions to food packaging, Nat. Sustain. 6 (4) (2023) 360–367.
[2] K.Y. Perera, A.K. Jaiswal, S. Jaiswal, Biopolymer-based sustainable food packaging materials: challenges, solutions, and applications, Foods 12 (12) (2023) 2422.
[3] Y.A. Shah, S. Bhatia, A. Al-Harrasi, T.S. Khan, Advancements in the biopolymer films for food packaging applications: a short review, Biotechnol. Sustain. Mater. 1 (1) (2024) 2.
[4] J. O'Loughlin, D. Doherty, B. Herward, C. McGleenan, M. Mahmud, P. Bhagabati, J. Gaughran, et al., The potential of bio-based polylactic acid (PLA) as an alternative in reusable food containers: a review, Sustainability 15 (21) (2023) 15312.
[5] A.P. D'Almeida, T.L. de Albuquerque, Innovations in food packaging: from bio-based materials to smart packaging systems, Processes 12 (10) (2024) 2085.
[6] M. Ghasemlou, C.J. Barrow, B. Adhikari, The future of bioplastics in food packaging: an industrial perspective, Food Packag. Shelf Life 43 (2024) 101279.
[7] J. Sempere-Torregrosa, M.P. Arrieta, F. Dominici, D. Puglia, L. Torre, M.D. Samper, Biodegradable active packaging films reinforced with thyme waste nanoparticles, Discov. Food 5 (1) (2025) 360.
[8] R. Şomoghi, S. Mihai, F. Oancea, An overview of bio-based polymers with potential for food packaging applications, Polymers 17 (17) (2025) 2335.
[9] X. Shi, L. Cui, C. Xu, S. Wu, Next-generation bioplastics for food packaging: sustainable materials and applications, Materials 18 (12) (2025) 2919.
[10] S.A. Siddiqui, X. Yang, R.K. Deshmukh, K.K. Gaikwad, N.A. Bahmid, R. Castro-Muñoz, Recent advances in reinforced bioplastics for food packaging–a critical review, Int. J. Biol. Macromol. 263 (2024) 130399.
[11] I. Armentano, E. Fortunati, N. Burgos, F. Dominici, F. Luzi, S. Fiori, et al., Processing and characterization of plasticized PLA/PHB blends for biodegradable multiphase systems, Express Polym. Lett. 9 (7) (2015) 583–596.
[12] A.A. Barmpaki, U.C. Paul, M. Nardi, A. Athanassiou, Eco-friendly blends of polylactic acid and polyhydroxybutyrate enhanced with epoxidized soybean oil methyl ester for food-packaging applications, ACS Appl. Polym. Mater. 6 (15) (2024) 8997–9007.
[13] M.A. Abdelwahab, A. Flynn, B.Sen Chiou, S. Imam, W. Orts, E. Chiellini, Thermal, mechanical and morphological characterization of plasticized PLA–PHB blends, Polym. Degrad. Stab. 97 (9) (2012) 1822–1828.
[14] M.P. Arrieta, M.D. Samper, J. López, A. Jiménez, Combined effect of poly (hydroxybutyrate) and plasticizers on polylactic acid properties for film intended for food packaging, J. Polym. Environ. 22 (4) (2014) 460–470.
[15] J. Sempere-Torregrosa, J.M. Ferri, H. de la Rosa-Ramírez, C. Pavon, M.D. Samper, Effect of epoxidized and maleinized corn oil on properties of polylactic acid (PLA) and polyhydroxybutyrate (PHB) blend, Polymers 14 (19) (2022) 4205.
[16] S.J. Álvarez-Méndez, J.L. Ramos-Suárez, A. Ritter, J.M. González, Á.C. Pérez, Anaerobic digestion of commercial PLA and PBAT biodegradable plastic bags: potential biogas production and ^{1}H NMR and ATR-FTIR assessed biodegradation, Heliyon 9 (6) (2023).
[17] L. Senila, E. Kovacs, M. Senila, A review of polylactic acid (PLA) and poly (3-hydroxybutyrate)(PHB) as bio-sourced polymers for membrane production applications, Membranes 15 (7) (2025) 210.
[18] S. Taamallah, S. Douiri, S.M. Keshk, R. Ben Arfi, A. Ghorbal, K. Charradi, D. Ghorbel, et al., Comparative effects of various plasticizers on the physicochemical characteristics of polyhydroxybutyrate (PHB) film for food packaging, Polymers 17 (22) (2025) 3071.
[19] Ö.E. Yurt, N. Sen, H. Simsir, Y. Kucuk, E. Altas, M.S. Gok, M.H. Cetin, et al., Investigation of tribological performance of hydrothermal carbon by pin-on-disc test and warm deep drawing process, Surf. Topogr. Metrol. Prop. 12 (2) (2024) 025019.
[20] F. Barrino, H. De La Rosa-Ramírez, R. Finamore, S.F. Mirpoor, J.L. Martínez, C. Schiraldi, M.D. Samper, et al., Polybutylene succinate film incorporating essential oil as active packaging materials to prolong tomatoes shelf-life, Appl. Food Res. (2025) 101360.
[21] Z.A. Nur Hanani, Surface properties of biodegradable polymers for food packaging, in: Polymers for Food Applications, Springer International Publishing, Cham, 2018, pp. 131–147.
[22] M. Naeimirad, B. Krins, G.J.M. Gruter, A review on melt-spun biodegradable fibers, Sustainability 15 (19) (2023) 14474.
[23] F. Barrino, H. De La Rosa-Ramírez, R. Finamore, S.F. Mirpoor, J.L. Martínez, C. Schiraldi, M.D. Samper, Polybutylene succinate film incorporating essential oil as active packaging materials to prolong tomatoes shelf-life, Appl. Food Res. (2025) 101360.
[24] F. Barrino, G.M.L. Piccolo, J. Sempere-Torregrosa, H.D.L. Rosa-Ramírez, M. D. Samper, New food packaging material based on modified corn oil, Macromol. Symp. 414 (3) (2025) 70050.
[25] M.K. Patel, M. Zaccone, L. De Brauwer, R. Nair, M. Monti, V. Martinez-Nogues, K. Oksman, et al., Improvement of poly (lactic acid)-poly (hydroxy butyrate) blend properties for use in food packaging: processing, structure relationships, Polymers 14 (23) (2022) 5104.
[26] R. Şomoghi, S. Mihai, F. Oancea, An overview of bio-based polymers with potential for food packaging applications, Polymers 17 (17) (2025) 2335.
[27] K. Olonisakin, A.K. Mohanty, M. Thimmanagari, M. Misra, Recent advances in biodegradable polymer blends and their biocomposites: a comprehensive review, Green Chem. 27 (38) (2025) 11656–11704.
[28] S. Hussain, S. Berry, Bio-based starch blends in active food packaging applications, in: Nanomanufacturing Techniques in Sustainable Healthcare Applications, CRC Press, 2024, pp. 94–109.
[29] R. Scaffaro, A. Maio, F. Sutera, E.F. Gulino, M. Morreale, Degradation and recycling of films based on biodegradable polymers: a short review, Polymers 11 (4) (2019) 651.
[30] D. Kosmalska, K. Janczak, A. Raszkowska-Kaczor, A. Stasiek, T. Ligor, Polylactide as a substitute for conventional polymers—biopolymer processing under varying extrusion conditions, Environments 9 (5) (2022) 57.
[31] Cai, J. Abdullah, M.A. Hafeez, Q. Wang, S. Farooq, Q. Huang, J. Xiao, et al., Biopolymer-based functional films for packaging applications: a review, Front. Nutr. 9 (2022) 1000116.
[32] A. Ajji, L.A. Utracki, Interphase and compatibilization of polymer blends, Polym. Eng. Sci. 36 (12) (1996) 1574–1585.
[33] R. Trivedi, M. Raj, L. Raj, R. Patel, High-performance fiber-reinforced composites using cardanol-based resin and epoxy resin blend: mechanical, thermal, morphological, and chemical resistance properties with various hardeners, Compos. Interfaces (2025) 1–25.
[34] B.M. Trinh, D.T. Tadele, T.H. Mekonnen, Robust and high barrier thermoplastic starch–PLA blend films using starch-graft-poly (lactic acid) as a compatibilizer, Mater. Adv. 3 (15) (2022) 6208–6221.